

Supplementary information

We are well aware of the fact that our reduced minus oxidized difference spectra (Fig. 1) are dramatically different from those presented in previous investigations. For example in the typical FTIR-spectroscopy experiment on cytochrome c oxidase (see, for example: Rich PR, Breton J. Biochemistry 2002, 41, 967-973; Hellwig et al, Biochemistry 1998 37, 7390-9) the ratio of the amplitude of the absolute spectra, for example, in amide I band, to the maximal amplitude on the reduced-oxidized difference spectra obtained upon reduction and oxidation is about 1000. Moreover, the sum of all areas of all positive and negative peaks in the reduced minus oxidized spectra are the same.

By contrast, in our experiment, the absolute absorbance of the SEIRA spectrum of the CcO immobilized in the orientation with Cu A directed toward the electrode (His-tag attached to subunit II), is about 6×10^{-3} (Fig. 1)

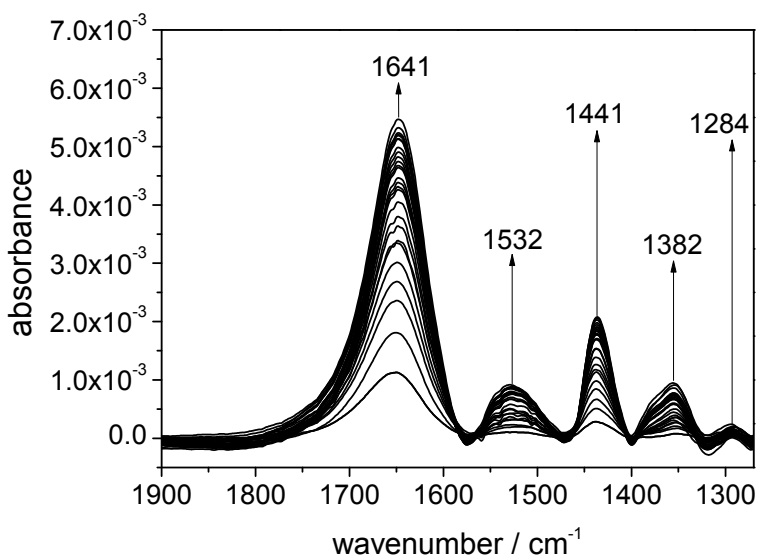


Fig. 1 Absorbance spectra of the CcO in the orientation with Cu A directed toward the electrode (His-tag attached to subunit II) as a function of time during immobilization, from bottom to top, without any potential applied. The band at 1441 cm^{-1} is due to the complexation of the Ni-NTA group

while the maximum absorbance of reduced –minus oxidized spectra (Fig. 1, main article) is in the same order of magnitude. Moreover, the sum of all areas of all positive and negative peaks in the reduced minus oxidized spectra are not the same as in earlier studies.

For an explanation, we have to take into account that we use direct electron transfer (ET) in conjunction with a different FTIR technique, namely surface-enhanced IR absorption spectroscopy (SEIRAS), whereas the data presented by other researchers were obtained under quite different conditions. For

example Rich and Breton (J. Biochemistry 2002, 41, 967-973) employ chemical reducing and oxidizing compounds such as tetramethyl-phenylenediamine mediated by phenazinemethosuphate (for reduction) and ferricyanide (for oxidation) on a detergent depleted sample that had been assembled on the ATR crystal in a random orientation. Hellwig et al. (Biochemistry 1998 37, 7390-9), on the other hand use electrochemical reduction/oxidation, however, in the presence of a cocktail of mediators, in conjunction with transmission FTIR in a thin layer cell.

In order to compare the different approaches, we performed a couple of control experiments, described in ref. 22. The first control experiment comprises a potentiometric titration in the presence of the same set of mediators as in Hellwig et al. (Biochemistry 1998 37, 7390-9). In addition, CcO was immobilized in the reverse orientation so that Cu_A is pointing away from the electrode and can only be reduced by mediators which carry electrons from the electrode to the redox center. The reduced-minus oxidized difference spectra obtained under these conditions are characterized by peaks and troughs such that the sum of all areas of all positive and negative peaks in the reduced minus oxidized spectra are the same equivalent to previously reported spectra in the literature (fig. 2).

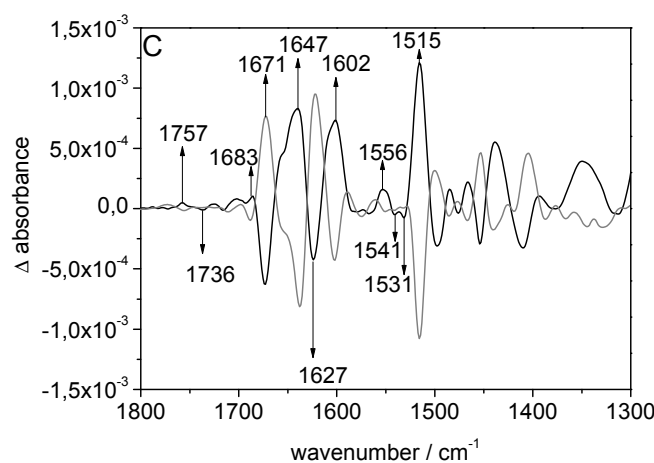


Fig. 2 Fully reduced vs. fully oxidized (black) and fully oxidized vs. fully reduced absorbance spectrum (grey) of CcO immobilized via His-tag on subunit I (cf. Fig. 1B) in the presence of mediators.

The maximum absorbance difference is around 1×10^{-3} , only about 6 times smaller than the absolute absorbance of the SEIRA spectrum of the CcO immobilized in the same orientation without any potential applied, Fig. 3

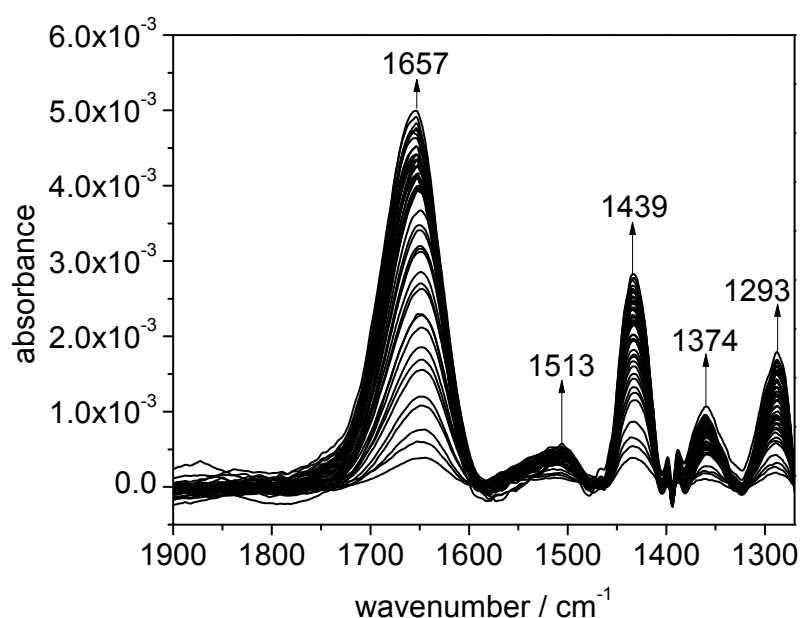


Fig. 3 Absorbance spectra of the CcO in the orientation with Cu A directed away from the electrode (His-tag attached to subunit I) as a function of time during immobilization, from bottom to top, without any potential applied. The band at 1439 cm⁻¹ is due to the complexation of the Ni-NTA group.

Hence the ratio of roughly 6:1 between absolute absorbance and reduced minus oxidized difference SEIRA spectrum is much lower than 1000:1 found in the publications mentioned above (Rich&Breton, Hellwig et al.) For an explanation we have to consider the extra enhancement effect of the applied electric field, described by the factor f_{EF} in eq. 1, which relates the absorbances A of SEIRA spectra with the molar absorption coefficient ε , the concentration c and the effective thickness d_{eff} of the protein layer, according to

$$A = \varepsilon c d_{eff} f_{EF} \quad (1)$$

The contribution of the electric field is known to be substantial, however, hard to discriminate from the general surface enhancement effect.

Further considering that ε is determined by the transition dipole moment, p , and its angle to the axis of the structural element, Θ , according to

$$\varepsilon \approx e^2 p^2 \cos^2 \Theta \quad (2)$$

where e is the electric field of the photon, absorbance changes can also be explained in terms of structural and orientational changes of the protein. Different oxidation states are expected to affect the structure of the protein, particularly since amino acids identified by IR are very close to the redox centers whereas different orientations affect the transition dipole moment. The angle between the

transition dipole moment of the amid I vibration and the axis of a α -helical structure may vary between 29° and 40°. The α -helices are already pre-oriented due to the immobilization method (Fig. 4B). As a consequence of ET (even mediated ET) all of them should change the orientation of the C=O groups in the same direction. As a result strong absorbance changes could be expected, considering that only molecules contribute to the SEIRAS effect, whose transition dipole moments are oriented in the z-direction.

However, these effects do not explain the overall appearance of the reduced –minus-oxidized difference spectra measured under conditions of direct ET (Fig. 1, main article), which are fundamentally different from the ones measured under conditions of mediated ET (Fig. 2). In the first case, the peaks are almost unidirectional whereas in the second case the sum of all areas of all positive and negative peaks in the reduced minus oxidized spectra are the same. For an explanation, we have to consider that direct ET is highly likely to occur via a sequential mechanism according to modelling studies of cyclic voltammograms. (Schach et al., Modeling Direct Electron Transfer to a Multi-Redox Center Protein: Cytochrome c Oxidase, *J. Electroanal. Chem.* **649** (2010) 268–276)

Hence electrons will be transferred along the unique tunnelling pathway from the electrode along the spacer to Cu_A and through the protein from one redox center to the next. As a result a large dipole moment will be generated within the protein matrix on reduction. Vibrations of strongly polarized groups within adsorbed molecules give larger enhancements than other groups, which was explained by donor-acceptor interactions with the metal. (G. T. Merklin and P. R. Griffiths, *Langmuir*, 1997, 13, 6159-6163., M. Osawa, *Handbook of Vibrational Spectroscopy*, John Wiley & sons, San Francisco, 2002.) Charge oscillations between molecular orbitals and the metal were considered to increase the absorption coefficient of the adsorbate. (B. N. J. Persson and A. Liebsch, *Surf Sci*, 1981, 110, 356-368).

The increase will be unidirectional, particularly if the polarization increases stepwise in one direction and the polarized groups are highly oriented with respect to the surface. This explanation is in line with the observation of positive bands on reduction (black curves in Fig. 3A, B in ref 22) and negative bands on oxidation (grey curves in Fig. 3A, B in ref 22) . This would explain why we end up at absorbances around 5×10^{-3} , still higher than 1×10^{-3} obtained for the spectra obtained from mediated ET.

Finally, another effect to be taken into account is unspecific absorbance changes reflecting conformational changes and/or polarizations of the protein in the electric field which are not due to redox processes. In order to check this effect the second control experiment was performed. It comprises a potentiometric titration of the CcO in the orientation with Cu_A pointing away from the electrode surface, i.e. immobilized via His-tag on subunit I, however, with no mediators added. Hence in this case both mediated as well as direct ET is prohibited. Hence only unspecific absorbance changes are recorded due to peptide groups affected by the electric field in the absence of any real heterogenous ET. For a detailed analysis of the data as compared to the data obtained under conditions

of direct ET we refer to ref 22 and Fig. 7 therein. We can deduce that about one third of the absorbance difference of the reduced vs. oxidized spectra is due to unspecific absorption.

Fig. 7 of ref 22 is repeated here for comparison purposes (note that band areas are plotted rather than band amplitudes, hence a direct comparison with Fig. 1-3 is not possible)

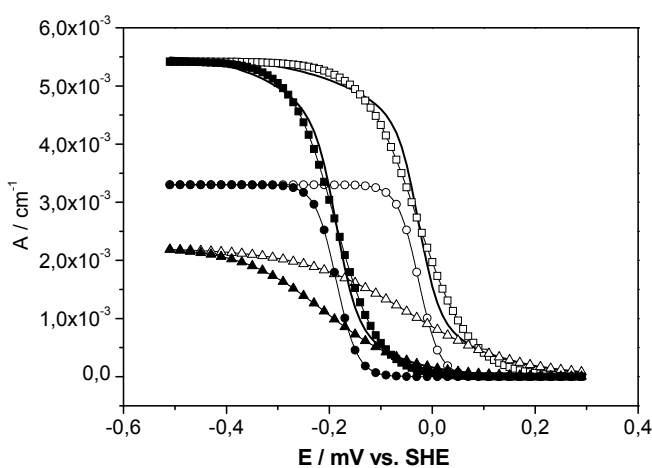


Fig. 7 of ref. 22. Redox-related and unspecific contribution to the dependence of band area A on applied potential E . Band at 1605 cm^{-1} of activated CcO (cf. Fig. 2D in ref 22), data calculated as explained in the text (squares); the solid line represents eq. 3 fitted to these data, which comprises a redox-related (circles) and an unspecific contribution (triangles). Open and closed symbols pertain oxidative and reductive titration, respectively. For graphical reasons the curves for the oxidative titration are shifted so that they converge to zero at high potentials.

In summary we can conclude that using SEIRAS under the influence of electric fields the direct comparison of absolute and reduced –minus–oxidized difference spectra is not feasible. Hence an estimate as to the extent of the conformational changes as a function of redox transitions is not possible from our experiments.

Analysis of the 2D-SEIRA spectra according to the rules of Noda

In the main article it was mentioned that the direction of the cross peaks in the asynchronous 2D-SEIRA spectra reveal information about the sequential order of the conformational transitions as a function of potential of different amino acids and secondary structures of peptide groups. Cross peaks in the asymmetric spectra of every two bands in Figs. 2B, 3B were analyzed according to the rules of Noda and compared with the direction of cross peaks in the synchronous spectra (Fig. 2A, 3A). This way the sequential order of a large number of correlated peaks was isolated and collected in Table 1 and 2

Table 1

Sequential order of vibrational modes obtained from the analysis of cross peaks in the **amide I region** according to the rules of Noda (references 26,27,46 main article), tentative band assignments according to references (9-15 main article). Amino acid are given in *R. sphaeroides* numbering

wave-number / cm ⁻¹	redox center	tentative band assignments	sequential order	
			activated	non-activated
1565; 1586	heme a ₃ ; CuA	Trp-NH; v(CC), δ(CH); W172, propionate; HisH; v(C=C); H260, H217; Arg-H ₅ ⁺ ; v _{as} (CN ₃ H ₅ ⁺); R481; Asp-COO ⁻ ; v _{as} (COO ⁻); D214	simultaneous	
1565; 1600	heme a ₃ ; CuA	Trp-NH; v(CC), δ(CH); W172, propionate; amide I β-sheet, v(C=O)	simultaneous	
1565; 1654	heme a ₃ ; heme a ₃ / CuA	Trp-NH; v(CC), δ(CH); W172, propionate; amide I α-helix, v(C=O)	1565 before 1654	
1565; 1742	heme a ₃ ; heme a	Trp-NH; v(CC), δ(CH); W172, propionate; Glu- COOH; v(C=O); E286	simultaneous	
1574; 1620	heme a & a ₃ ; heme a ₃	propionate (deprot.); Tyr-OH; v(CC), δ(CH); Y288; v(CC), v(C=C); W280, W172; vinyl; v(C-C), amide I β-sheet, v(C=O)		simultaneous
1574; 1656	heme a & a ₃ ; heme a ₃ / CuA	propionate (deprot.); amide I α-helix, v(C=O)		simultaneous
1586; 1600	CuA; CuA	HisH; v(C=C); H260, H217; Arg-H ₅ ⁺ ; v _{as} (CN ₃ H ₅ ⁺); R481; Asp-COO ⁻ ; v _{as} (COO ⁻); D214; amide I β-sheet, v(C=O)	simultaneous	
1586; 1623	CuA; heme a ₃	HisH; v(C=C); H260, H217; Arg-H ₅ ⁺ ; v _{as} (CN ₃ H ₅ ⁺); R481; Asp-COO ⁻ ; v _{as} (COO ⁻); D214; Tyr-OH; v(CC), δ(CH); Y288; v(CC), v(C=C); W280, W172; vinyl; v(C-C), amide I β-sheet, v(C=O)	simultaneous	
1586; 1654	CuA; heme a ₃ / CuA	HisH; v(C=C); H260, H214; Arg-H ₅ ⁺ ; v _{as} (CN ₃ H ₅ ⁺); R481; Asp-COO ⁻ ; v _{as} (COO ⁻); D214; amide I α-helix, v(C=O)	1586 before 1654	
1586; 1742	CuA; heme a	HisH; v(C=C); H260, H214; Arg-H ₅ ⁺ ; v _{as} (CN ₃ H ₅ ⁺); R481; Asp-COO ⁻ ; v _{as} (COO ⁻); D214; Glu-COOH; v(C=O); E286	simultaneous	
1600; 1623	CuA; heme a ₃	amide I β-sheet, v(C=O); Tyr-OH; v(CC), δ(CH); Y288; v(CC), v(C=C); W280, W172; vinyl; v(C-C), amide I β-sheet, v(C=O)	simultaneous	
1600; 1654	CuA; heme a ₃ / CuA	amide I β-sheet, v(C=O); amide I α-helix, v(C=O)	1654 before 1600	
1600; 1742	CuA; heme a	amide I β-sheet, v(C=O); Glu-COOH; v(C=O); E286	simultaneous	
1607; 1639	CuA; heme a ₃	amide I β-sheet, v(C=O); formyl, v(C=O), amide I β-sheet, v(C=O)		simultaneous
1620; 1656	heme a ₃ ; heme a ₃ / CuA	Tyr-OH; v(CC), δ(CH); Y288; v(CC), v(C=C); W280, W172; vinyl; v(C-C), amide I β-sheet, v(C=O); amide I α-helix, v(C=O)		1620 before 1656
1620; 1742	heme a ₃ ; heme a	Tyr-OH; v(CC), δ(CH); Y288; v(CC), v(C=C); W280, W172; vinyl; v(C-C), amide I β-sheet, v(C=O); Glu-COOH; v(C=O); E286		simultaneous

wave-number / cm ⁻¹	redox center	tentative band assignments	sequential order	
			activated	non-activated
1623; 1654	heme a ₃ ; heme a ₃ / CuA	Tyr-OH; ν(CC), δ(CH); Y288; ν(CC), ν(C=C); W280, W172; vinyl; ν(C-C), amide I β-sheet, ν(C=O); amide I α-helix ν(C=O)	1654 before 1623	
1623; 1742	heme a ₃ ; heme a	Tyr-OH; ν(CC), δ(CH); Y288; ν(CC), ν(C=C); W280, W172; vinyl; ν(C-C), amide I β-sheet, ν(C=O); Glu-COOH; ν(C=O); E286	simultaneous	
1639; 1681	heme a ₃ ; CuA	formyl, ν(C=O), amide I β-sheet, ν(C=O); amide I β-sheet, ν(C=O)		simultaneous
1654; 1742	heme a ₃ / CuA; heme a	amide I α-helix, ν(C=O); Glu-COOH; ν(C=O); E286	1742 before 1654	
1682; 1700	CuA; heme a₃	amide I β-sheet, ν(C=O); amide I β-turn	simultaneous	

Table 2

Sequential order of vibrational modes obtained from the analysis of cross peaks in the **fingerprint region** according to the rules of Noda (references 26,27,46 main article), tentative band assignments according to references (9-15 main article). Amino acid are given in *R. sphaeroides* numbering

wave-number / cm ⁻¹	redox center	tentative band assignments	sequential order	
			activated	non-activated
1326; 1389	CuB; heme a	$\delta(\text{CH})$; W280; Tyr-O ⁻ ; $\delta(\text{CH}_2)$, $\nu(\text{CC})$, $\delta(\text{CH})$; Y288; Asp-COOH; $\delta(\text{COH})$; D407; $\delta(\text{COH})$, $\delta(\text{CH})$; T352; $\delta(\text{COH})$; $\delta(\text{CH})$; T48; $\gamma_{\omega}(\text{CH}_2)$; E254; propionate	1326 before 1389	
1326; 1402	CuB; CuA	$\delta(\text{CH})$; W280; Tyr-O ⁻ ; $\delta(\text{CH}_2)$, $\nu(\text{CC})$, $\delta(\text{CH})$; Y288; Asp-COOH; $\delta(\text{COH})$; D407; $\delta(\text{COH})$, $\delta(\text{CH})$; T352; Glu-COO ⁻ ; $\nu_s(\text{COO}^-)$; E254; Asp-COO ⁻ ; $\nu_s(\text{COO}^-)$; D214; Trp-NH; $\nu(\text{CC})$, $\delta(\text{NH})$, $\delta(\text{CH})$; W143	simultaneous	
1326; 1424	CuB; CuA	$\delta(\text{CH})$; W280; Tyr-O ⁻ ; $\delta(\text{CH}_2)$, $\nu(\text{CC})$, $\delta(\text{CH})$; Y288; Asp-COOH; $\delta(\text{COH})$; D407; $\delta(\text{COH})$, $\delta(\text{CH})$; T352; Trp-NH; $\delta(\text{NH})$, $\nu(\text{CC})$, $\nu(\text{CH})$; W143; HisH; $\nu(\text{CN})$, $\delta(\text{NH})$; $\delta_s(\text{CH}_x)$; H217, H260; Asp-COOH; $\delta(\text{COH})$; D214	simultaneous	
1326; 1434	CuB; CuA	$\delta(\text{CH})$; W280; Tyr-O ⁻ ; $\delta(\text{CH}_2)$, $\nu(\text{CC})$, $\delta(\text{CH})$; Y288; Asp-COOH; $\delta(\text{COH})$; D407; $\delta(\text{COH})$, $\delta(\text{CH})$; T352; Trp-NH; $\delta(\text{CH})$, $\nu(\text{CC})$, $\nu(\text{CN})$; W143; Asp-COOH; $\delta(\text{COH})$; D214; Glu-COO ⁻ ; $\nu_s(\text{COO}^-)$; E254	1326 before 1434	
1326; 1450	CuB; CuB	$\delta(\text{CH})$; W280; Tyr-O ⁻ ; $\delta(\text{CH}_2)$, $\nu(\text{CC})$, $\delta(\text{CH})$; Y288; Asp-COOH; $\delta(\text{COH})$; D407; $\delta(\text{COH})$, $\delta(\text{CH})$; T352; His ⁻ ; H334, H333, H284	simultaneous	
1326; 1483	CuB; CuB	$\delta(\text{CH})$; W280; Tyr-O ⁻ ; $\delta(\text{CH}_2)$, $\nu(\text{CC})$, $\delta(\text{CH})$; Y288; Asp-COOH; $\delta(\text{COH})$; D407; $\delta(\text{COH})$, $\delta(\text{CH})$; T352; Trp-NH; $\nu(\text{CC})$, $\delta(\text{CH})$; W280	1326 before 1483	
1326; 1495	CuB; CuB	$\delta(\text{CH})$; W280; Tyr-O ⁻ ; $\delta(\text{CH}_2)$, $\nu(\text{CC})$, $\delta(\text{CH})$; Y288; Asp-COOH; $\delta(\text{COH})$; D407; $\delta(\text{COH})$, $\delta(\text{CH})$; T352; $\nu(\text{CC})$, $\delta(\text{CH})$; W280; HisH; $\nu(\text{C=N})$, $\delta(\text{CH})$; H333, H334	1326 before 1495	
1326; 1528	CuB; heme a₃	$\delta(\text{CH})$; W280; Tyr-O ⁻ ; $\delta(\text{CH}_2)$, $\nu(\text{CC})$, $\delta(\text{CH})$; Y288; Asp-COOH; $\delta(\text{COH})$; D407; $\delta(\text{COH})$, $\delta(\text{CH})$; T352; propionate heme; ν_{38s} ; heme; ν_{38y}	1326 before 1528	
1330; 1436	CuB; CuA	$\gamma_{\omega}(\text{CH}_2)$; W280; Tyr-O ⁻ ; $\gamma_{\omega}(\text{CH}_2)$; Y288; Asp-COOH; $\delta(\text{COH})$; D407; $\delta(\text{COH})$, $\delta(\text{CH})$; T352; Trp-NH; $\delta(\text{CH})$, $\nu(\text{CC})$, $\nu(\text{CN})$; W143; Asp-COOH; $\delta(\text{COH})$; D214; Glu-COO ⁻ ; $\nu_s(\text{COO}^-)$; E254		1330 before 1436
1344; 1436	heme a₃ , CuA	?; Trp-NH; $\delta(\text{CH})$, $\nu(\text{CC})$, $\nu(\text{CN})$; W143; Asp-COOH; $\delta(\text{COH})$; D214; Glu-COO ⁻ ; $\nu_s(\text{COO}^-)$; E254		1344 before 1436
1344; 1470	heme a₃ , heme a₃	ν_4 ; ν_3		simultaneous

wave-number / cm ⁻¹	redox center	tentative band assignments	sequential order	
			activated	non-activated
1357; 1436	heme a ₃ ; CuA	v(CC), v(CN), δ(CH); W172, W280; γ _ω (CH ₂); Y288; v ₄ ; Trp-NH; δ(CH), v(CC), v(CN); W143; Asp-COOH; δ(COH); D214; Glu-COO ⁻ ; v _s (COO ⁻); E254		simultaneous
1388; 1402	heme a; CuA	δ(COH); δ(CH); T48; γ _ω (CH ₂); E286; propionate; Glu-COO ⁻ ; v _s (COO ⁻); E254; Asp-COO ⁻ ; v _s (COO ⁻); D214; Trp-NH; v(CC), δ(NH), δ(CH); W143	1402 before 1388	
1388; 1424	heme a; CuA	δ(COH); δ(CH); T48; γ _ω (CH ₂); E286; propionate; Trp-NH; δ(NH), v(CC), v(CH); W143; HisH; v(CN), δ(NH); δ _s (CH _x); H217, H260; Asp-COOH; δ(COH); D214	1424 before 1388	
1388; 1434	heme a; CuA	δ(COH); δ(CH); T48; γ _ω (CH ₂); E286; propionate; Trp-NH; δ(CH), v(CC), v(CN); W143; Asp-COOH; δ(COH); D214; Glu-COO ⁻ ; v _s (COO ⁻); E254	1388 before 1434	
1388; 1450	heme a; CuB	δ(COH); δ(CH); T48; γ _ω (CH ₂); E286; propionate; His ⁻ ; H334, H333, H284	simultaneous	
1388; 1483	heme a; CuB	δ(COH); δ(CH); T48; γ _ω (CH ₂); E286; propionate; Trp-NH; v(CC), δ(CH); W280	simultaneous	
1388; 1495	heme a; CuB	δ(COH); δ(CH); T48; γ _ω (CH ₂); E286; propionate; v(CC), δ(CH); W280; HisH; v(C=N), δ(CH); H333, H334	1495 before 1388	
1388; 1528	heme a; heme a ₃	δ(COH); δ(CH); T48; γ _ω (CH ₂); E286; propionate; heme; v _{38s} ; heme; v _{38y}	1528 before 1388	
1389; 1469	heme a; CuA	δ(COH); δ(CH); T48; γ _ω (CH ₂); E286; propionate; Trp-NH; δ(CH), v(CC), v(CN); W143		1469 before 1389
1402; 1424	CuA; CuA	Glu-COO ⁻ ; v _s (COO ⁻); E254; Asp-COO ⁻ ; v _s (COO ⁻); D214; Trp-NH; v(CC), δ(NH), δ(CH); W143; Trp-NH; δ(NH), v(CC), v(CH); W143; HisH; v(CN), δ(NH); δ _s (CH _x); H217, H260; Asp-COOH; δ(COH); D214	simultaneous	
1402; 1434	CuA; CuA	Glu-COO ⁻ ; v _s (COO ⁻); E254; Asp-COO ⁻ ; v _s (COO ⁻); D214; Trp-NH; v(CC), δ(NH), δ(CH); W143; Trp-NH; δ(CH), v(CC), v(CN); W143; Asp-COOH; δ(COH); D214; Glu-COO ⁻ ; v _s (COO ⁻); E254	simultaneous	
1402; 1450	CuA; CuB	Glu-COO ⁻ ; v _s (COO ⁻); E254; Asp-COO ⁻ ; v _s (COO ⁻); D214; Trp-NH; v(CC), δ(NH), δ(CH); W143; His ⁻ ; H334, H333, H284	1450 before 1402	
1402; 1483	CuA; CuB	Glu-COO ⁻ ; v _s (COO ⁻); E254; Asp-COO ⁻ ; v _s (COO ⁻); D214; Trp-NH; v(CC), δ(NH), δ(CH); W143; Trp-NH; v(CC), δ(CH); W280	simultaneous	
1402; 1495	CuA; CuB	Glu-COO ⁻ ; v _s (COO ⁻); E254; Asp-COO ⁻ ; v _s (COO ⁻); D214; Trp-NH; v(CC), δ(NH), δ(CH); W143; v(CC), δ(CH); W280; HisH; v(C=N), δ(CH); H333, H334	1402 before 1495	

wave-number / cm ⁻¹	redox center	tentative band assignments	sequential order	
			activated	non-activated
1402; 1528	CuA; heme a₃	Glu-COO ⁻ ; v _s (COO ⁻); E254; Asp-COO ⁻ ; v _s (COO ⁻); D214; Trp-NH; v(CC), δ(NH), δ(CH); W143; propionate; heme; v _{38s} ; heme; v _{38y}	1402 before 1528	
1412; 1424	CuA; CuA	Glu-COO ⁻ ; v _s (COO ⁻); E254; Asp-COO ⁻ ; v _s (COO ⁻); D214; Trp-NH; v(CC), δ(NH), δ(CH); W143; Trp-NH; δ(NH), v(CC), v(CH); W143; HisH; v(CN), δ(NH); δ _s (CH _x); H217, H260; Asp-COOH; δ(COH); D214	simultaneous	
1424; 1450	CuA; CuB	Trp-NH; δ(NH), v(CC), v(CH); W143; HisH; v(CN), δ(NH); δ _s (CH _x); H217, H260; Asp-COOH; δ(COH); D214; His ⁻ ; H334, H333, H284	1424 before 1450	
1434; 1450	CuA; CuB	Trp-NH; δ(CH), v(CC), v(CN); W143; Asp-COOH; δ(COH); D214; Glu-COO ⁻ ; v _s (COO ⁻); E254; His ⁻ ; H334, H333, H284	1450 before 1434	
1434; 1483	CuA; CuB	Trp-NH; δ(CH), v(CC), v(CN); W143; Asp-COOH; δ(COH); D214; Glu-COO ⁻ ; v _s (COO ⁻); E254; Trp-NH; v(CC), δ(CH); W280	1434 before 1483	
1434; 1495	CuA; CuB	Trp-NH; δ(CH), v(CC), v(CN); W143; Asp-COOH; δ(COH); D214; Glu-COO ⁻ ; v _s (COO ⁻); E254; v(CC), δ(CH); W280; HisH; v(C=N), δ(CH); H333, H334	1434 before 1495	
1434; 1528	CuA; heme a₃	Trp-NH; δ(CH), v(CC), v(CN); W143; Asp-COOH; δ(COH); D214; Glu-COO ⁻ ; v _s (COO ⁻); E254; propionate; heme; v _{38s} ; heme; v _{38y}	1528 before 1434	
1436; 1502	CuA; CuA	Trp-NH; δ(CH), v(CC), v(CN); W143; Asp-COOH; δ(COH); D214; Glu-COO ⁻ ; v _s (COO ⁻); E254; ?		simultaneous
1436; 1510	CuA; CuA	Trp-NH; δ(CH), v(CC), v(CN); W143; Asp-COOH; δ(COH); D214; Glu-COO ⁻ ; v _s (COO ⁻); E254; Trp-NH; v(CN), δ(CH), δ(NH); W143		1510 before 1436
1436; 1517	CuA; CuA	Trp-NH; δ(CH), v(CC), v(CN); W143; Asp-COOH; δ(COH); D214; Glu-COO ⁻ ; v _s (COO ⁻); E254; ?		simultaneous
1436; 1545	CuA; heme a	Trp-NH; δ(CH), v(CC), v(CN); W143; Asp-COOH; δ(COH); D214; Glu-COO ⁻ ; v _s (COO ⁻); E254; heme v _{38y}		unknown
1450; 1483	CuB; CuB	His ⁻ ; H333, H334, H284; Trp-NH; v(CC), δ(CH); W280	simultaneous	
1450; 1495	CuB; CuB	His ⁻ ; H334, H333, H284; v(CC), δ(CH); W280; HisH; v(C=N), δ(CH); H333, H334	simultaneous	
1450; 1528	CuB; heme a₃	His ⁻ ; H334, H333, H284; propionate; heme; v _{38s} ; heme; v _{38y}	1528 before 1450	
1483; 1495	CuB; CuB	Trp-NH; v(CC), δ(CH); W280; v(CC), δ(CH); W280; HisH; v(C=N), δ(CH); H333, H334	simultaneous	
1483; 1528	CuB; heme a₃	Trp-NH; v(CC), δ(CH); W280; propionate; heme; v _{38s} ; heme; v _{38y}	simultaneous	
1495; 1528	CuB; heme a₃	v(CC), δ(CH); W280; HisH; v(C=N), δ(CH); H333, H334; propionate; heme; v _{38s} ; heme; v _{38y}	simultaneous	